Published in final edited form as:
*J Immunol*. 2009 March 1; 182(5): 2726–2737. doi:10.4049/jimmunol.0803479.

# Antigen processing and MHC-II presentation by dermal and tumor infiltrating DC

**Michael Y. Gerner** and **Matthew F. Mescher**
Center for Immunology, University of Minnesota, Minneapolis, MN, 55455, US

## Abstract

MHC-II presentation by DC is necessary both for initial priming of CD4 T cells and for induction of peripheral effector function. While CD4 T cells can be critical for competent immunization-mediated cancer immunosurveillance, unmanipulated CD4 T cell responses to poorly immunogenic tumors result in either complete ignorance or tolerance induction, suggesting inadequate DC function. Here, we investigated the phenotype, antigen uptake and MHC-II presentation capacity of normal dermal DC and tumor infiltrating DC (TIDC) in both lymphoid and peripheral sites. We found that murine tumors were extensively infiltrated by partially activated TIDC that closely resembled dermal DC by surface marker expression. However, in contrast to dermal DC, TIDC were inefficient at MHC-II presentation due to poor intrinsic protein uptake capability. This resulted in both inferior initiation of T cell responses in the draining lymph node (DLN) and poor peripheral effector cell accumulation. In addition, toll-like receptor stimulation selectively enhanced MHC-II presentation of antigen by dermal DC but not TIDC in the DLN, and did not affect overall peripheral antigen uptake of either. These results show that TIDC are functionally distinct from normal interstitial DC, thus indicating that neoplastic tissues can evade effector CD4 T cells through modification of DC competence.

### Keywords

Dendritic Cells; T cells; Antigen Presentation/Processing; Tumor Immunity; Skin

## Introduction

Cancer immunosurveillance can be mediated through multiple mechanisms that involve cells of the adaptive and innate immune system (1). While CD8 T cells and NK cells have been the primary focus of cancer immunology due to direct cytolytic capabilities, CD4 T cells have recently been implicated as a critical cell type for successful immunosurveillance in vaccination and lymphopenia induced cancer therapy models (2–6). CD4 T cells have been shown to mediate indirect and direct anti-tumor effects through a multitude of cell contact and cytokine dependent mechanisms. Initial CD4 T cell activation in the DLN leads to upregulation of CD40L surface expression, which through binding of CD40 on DC causes DC maturation, increased DC longevity, production of guidance chemokines and initiation of 3$^{rd}$ signal cytokine production to support CD8 T cell activation (7–13). In addition, CD4 T cells are considered to be an important source of IL-2, necessary for continued effector CD8 T cell expansion as well as for formation of functional CD8 T cell memory (8,14,15). It has also been shown that effector CD4 T cells can greatly enhance CD8 T cell tumor infiltration after immunization (6). Together these helper effects have been proven necessary for optimal

Corresponding Author: Matthew F. Mescher, Mailing Address: Lab, Medicine and Pathology, Mayo Mail Code 334, 420 Delaware St SE, Minneapolis, MN, 55455, Phone: 612-626-2368, Fax: 612-625-2199, Email: E-mail: mesch001@umn.edu.

production and maintenance of effector and memory CD8 T cells, and therefore for direct CD8 T cell anti-tumor activity (2,3,6,13,16–21). In addition, effector CD4 T cells are capable of directly producing IFNγ, an inflammatory cytokine involved in enhancement of intratumoral (i.t.) chemokine expression and immune cell recruitment, activation of DC and macrophages, stabilization of surface MHC-I/II expression, induction of apoptosis, inhibition of tumor angiogenesis, as well as augmentation of CD8 T cell expansion (22–24). Through these indirect and direct anti-tumor effects CD4 T cells can orchestrate a comprehensive immunosurveillance program that can protect and treat diseased individuals.

In order for CD4 T cells to elicit effector function in 2º lymphoid and non-lymphoid peripheral tissues, such as cancerous tissues or infected sites, they need to be first activated by DLN DC presenting specific MHC-II-peptide complexes. The DLN DC are a heterogeneous mix of LN-resident as well as recent tissue-migrant DC populations that have differing abilities to present proteins to CD4 and CD8 T cells (25). It has been shown that while both LN-resident and migratory interstitial DC can activate CD4 T cells, migratory DC carry greater levels of antigen (Ag) and display a mature phenotype that allows full effector CD4 T cell activation and prolonged CD40L expression (12,25–28). It is thought that subsequent CD4 T cell DC interactions, which are necessary for continued CD4 T cell expansion and differentiation, allow licensing of immature LN-resident DC for complete maturation (29). Thus, CD4 T cells have the potential to license $CD8\alpha^+$ DC, the only DC subset shown to be efficient at processing peripheral proteins for cross-presentation on MHC-I, direct presentation on MHC-II, and production of high levels of cytokines necessary for CD8 T cell effector programming (8,19, 30–32). After migration out of 2º lymphoid organs into peripheral target tissues, effector CD4 T cells again need to see the specific MHC-II-peptide complexes to be stimulated to produce effector cytokines and to accumulate to large numbers ((33), McLachlan and Jenkins, personal communication). Considering that most parenchymal and cancerous tissues do not express MHC-II, stimulation of CD4 T cell at these sites critically depends on infiltrating interstitial DC, and not on macrophages, that can acquire proteins through various phagocytic mechanisms and present epitopes on MHC-II following lysosomal degradation ((34), McLachlan and Jenkins). Therefore, maximal anti-tumor CD4 T cell activity requires presentation of tumor-specific proteins by Ag-presenting cells in both DLN and inside the tumor. However, the capacity and kinetics of *in vivo* peripheral Ag uptake, processing, MHC-II presentation and DC migration for both normal interstitial DC as well as TIDC are poorly understood.

We, as well as others, have recently shown that while tumor-specific CD8 T cells were readily primed in the DLN of s.c. B16 melanoma and EL4 thymoma tumors, CD4 T cells remained completely ignorant of the progressing disease (35,36). The lack of CD4 T cell activation thus prevented licensing of immature DLN-resident $CD8\alpha^+$ DC that were cross-presenting tumor-specific proteins on MHC-I, and therefore contributed to the ensuing CD8 T cell tolerance induction (35). We found that the absence of CD4 T cell responses was not due to general T cell unresponsiveness in tumor-bearing animals, but due to tumor-mediated inhibition of MHC-II presentation of both tumor-secreted and i.t. injected proteins in DLN DC, as compared to normal s.c. protein inoculations (35). Considering that proteins from non-lymphoid peripheral sites are delivered and presented to CD4 T cells to a large extent by migratory DC, we hypothesized that Ag handling and/or migration of TIDC to DLN were defective (26). Even though TIDC have been shown capable of *ex vivo* protein uptake and presentation to both CD4 and CD8 T cells after s.c. immunization, we previously observed that TIDC were unable to present tumor-specific proteins acquired directly *in vivo* to CD4 T cells, arguing that steady state MHC-II presentation is defective in these cells (35,37). In addition, defects in DC differentiation leading to poor maturation and cytokine secretion in steady state and adjuvant-stimulated conditions have been described for human and murine neoplastic disease in both tumor-associated DC and TIDC (38–40).

To better understand the defects in tumor-Ag presentation to CD4 T cells, we have characterized the kinetics of Ag uptake, processing, MHC-II presentation and DC migration for both normal interstitial dermal DC and TIDC from poorly immunogenic tumors. Elucidation of the unmanipulated as well as adjuvant-stimulated Ag handling and migratory properties of TIDC *in vivo* provides insight into the first stages of the innate and adaptive immune system cross talk during cancer progression and after therapeutic immunization. This information is valuable for understanding the basis for the behavior and anti-tumor activity of responding tumor-specific T cells, and may ultimately be useful for diagnostic as well as therapeutic applications. In addition, dissection of normal interstitial DC function in peripheral tissues provides an improved perspective on peripheral CD4/DC interactions during s.c. immunizations, and has implications for DTH responses, as well as various bacterial and viral infections.

## Materials and Methods

### Mice, Tumor Cell Lines, and Adoptive Transfer

B16.F10 melanoma and EL.4 thymoma cell lines were maintained by *in vitro* culture in complete RPMI-1640 medium (cRPMI) (21). The B16.OVA melanoma line was maintained in cRPMI with 800 mg/ml G418 (Mediatech). The 4T1 breast cancer cell line was maintained in cRPMI supplemented with 2.5g/L glucose. Male C57BL/6Ncr mice (National Cancer Institute) were s.c. injected with $2\times10^5$ B16.F10 or B16.OVA cells, or with $2\times10^6$ EL.4 cells in PBS. Female Balb/cAnNCr mice (National Cancer Institute) were injected in the mammary fat pad with $5\times10^4$ 4T1 cells in PBS. $OVA_{257–264}$/H-$2K^b$ specific, TCR transgenic OT-I mice and $OVA_{323–339}$/I-Ab specific, TCR transgenic OT-II mice were a gift from Dr. Francis Carbone, U. of Melbourne, Australia. OT-I.PL and OT-II.PL mice were generated through crossing OT-I or OT-II mice with Thy1-congenic B6.PL-Thy1a/Cy (Thy1.1) mice (Jackson Laboratory) and breeding to homozygosity. OT-II.PL Rag 1−/− were generated by crossing OT-II.PL to C57BL/6J-recombinase-activating gene 1 (Rag1)tm1Mom (Rag1-deficient, 2216) mice (Jackson Laboratory). In some experiments, $1\times10^6$ naïve OT-I.PL cells, greater than 95% purity (21), and OT-II.PL Rag 1−/− were intravenously (i.v.) injected into animals one day prior to tumor inoculation. Experiments were conducted under specific pathogen-free conditions at the University of Minnesota, and were performed in compliance with relevant laws and institutional guidelines and with the approval of the Institutional Animal Care and Use Committee at the University of Minnesota (Minneapolis, MN).

### Protein and Adjuvant Injections

*E.Coli* expressing EαGFP was a kind gift of Dr. Marc Jenkins. The EαGFP protein was purified from bacterial lysates using a Nickel resin His-Bind column (Novagen) as previously described (26). Contaminating endotoxin was removed using TritonX-114 (MP Biomedicals) phase separation and SM-2 Bio Beads (Bio-Rad Labs). Protein was injected s.c. into naïve animals or directly i.t. (50μl volume) into day-10 B16.F10-bearing animals. Where indicated, EαGFP was injected into day-8 EL.4 and day-14 4T1 tumors. 35μg of CpG 1826 (Coley Pharmaceuticals), 50μg of *E.Coli* LPS (Sigma-Aldrich), or 35μg Poly-IC (Amersham Biosciences) were injected with the protein in some experiments. In some experiments, $5\times10^8$ 1μM unmodified red fluospheres (Invitrogen) were injected. For immunizations, 100μg OVA protein with 50μg LPS (Sigma-Aldrich) was injected i.v. into animals that were challenged with B16.F10 and B16.OVA on contra-lateral sides six days previously.

### Histology, Tissue Dissociation, and Flow Cytometry

8μm tissue sections were made of day 12–14 B16.F10 frozen tumor tissues using a CM1800 microtome (Leica Microsystems). Sections were fixed in acetone, air dried, and hydrated for 10 minutes in PBS. Sections were blocked with CD16/CD32 antibodies and 1% NMS PBS,

and stained with antibodies for CD11c, I-$A_b$, CD11b for 40 minutes. Sections were then washed and stained with 4',6-Diamindine-2'-phenylindole dihydrochloride (DAPI, Roche Apllied Science). Aqua Poly/Mount media (Polysciences) was then added to slides, which were then covered with Esco coverslips (Erie Scientific). Tissue sections were visualized on a Leica AF6000 microscope. For flow cytometric analysis of DC, LN or tumors of B16.F10-bearing mice were harvested and treated with 400 U/ml Collagenase D (Roche Applied Science) solution, and incubated for 25 min at 37° C. EDTA (10mM) was added for 1 minute, followed by a PBS wash. 1–3$cm^2$ shaved skin samples were incubated for two hours in complete RPMI-1640 medium, containing: 0.25 mg/ml bovine testes hyalurnidase, 0.1 mg/ml bovine pancreas deoxyribonuclease I, and 2.7 mg/ml collagenase from Clostridium histolyticum (Sigma-Aldrich). Dermis was disassociated by pipetting and washed with 2% FCS/PBS. Dendritic cells were identified by gating on $FSC^{high}$,$CD3^-$,$CD19^-$,$CD11c^+$,MHC-$II^+$,$CD11b^{+/-}$ populations. For immunization experiments, tissues were disrupted into single-cell suspensions through homogenization. Transferred OT-I.PL and OT-II.PL T cells were identified as $Thy1.1^+V\alpha2^+$ $CD8^+$ or $CD4^+$, respectively. All antibodies were obtained from eBiosciences, BD Biosciences, or Biolegend. Cell counts were obtained using PKH26 reference microbeads (Sigma-Aldrich). Cell density measurements were approximated by dividing the total cell number by an approximated tissue volume (LN - 27$mm^3$, skin - 100$mm^3$, day-10 tumor – 1000$mm^3$). All stained cells were collected on a LSR-II flow cytometer (BD Biosciences), and analyzed using FlowJo software (Treestar, Inc). Statistical significance was calculated by using unpaired two-tailed T-tests, unless indicated. P value representation: less than 0.05 are represented by one asterisk; less than 0.01 by two asterisks; less than 0.001 by three asterisks.

## Results

### Multiple transplantable tumor models inhibit MHC-II presentation in DLN DC

We previously found that i.t. injection of EαGFP fluorescent protein into B16.F10 melanoma resulted in lower numbers of both $GFP^+$ and MHC-II-peptide presenting DC in tumor DLN 24hrs post injection, in comparison to s.c. injection in normal mice (35). To test whether decreased Ag presentation in tumor DLN extended to other s.c. transplantable tumors , we injected EαGFP protein either s.c. into non-tumor bearing C57BL/6 or Balb/c animals, or i.t. into B16.F10 melanoma, EL4 thymoma, or 4T1 mammary carcinoma. We found that skin DLN contained a relatively large population of $GFP^+$ DC that were almost exclusively of the $CD11b^+$ mature migratory phenotype (Figure 1A, and data not shown). As expected, cell surface I-$A_b$-$E\alpha^{52–68}$ complex was only detected with the YAe antibody on the $GFP^+$ DC in the C57BL/6 skin DLN, and not in I-$A_E^+$ Balb/c skin and 4T1 tumor DLN. In sharp contrast to DC from s.c. injections, DLN from all of the tumors contained a smaller number of $GFP^+$ cells, as well as lower levels of YAe staining ( B16.F10 and EL4 tumors) (Figure 1A). Additionally, the cells that were $GFP^+$ in tumor DLN displayed a significantly lower levels of GFP compared to $GFP^+$ DC in skin DLN (Figure 1B). We did observe some experimental variability in the differences between B16.F10 and skin DLN in the numerous experiments that were done, which was most likely attributable to variations in drainage from the injected tumor site and the time required for dermal DC migration. Nonetheless, clear decreases in GFP MFI and MHC-II-peptide complex formation in the $GFP^+$ cells were observed in all experiments. These results showed that reduced DC-mediated Ag presentation in the tumor versus dermal DLN is a common feature of at least the three tumors examined here in two different mouse strains. This likely accounts for the complete CD4 T cell ignorance to either tumor-specific Ag or i.t. injected proteins that we previously observed (35).

### Tumors are infiltrated by a large number of partially activated CD11b$^+$ DC

Since migratory DC bring in the highest levels of peripheral proteins into the DLN, we hypothesized poor initial tumor infiltration by DC might account for diminshed numbers of DC migrants and hence the low level of Ag presentation found in tumor DLN (26). We therefore compared the numbers and phenotypes of DC present in the tumor and compared these to a 1×2cm patch of skin surrounding the s.c. injection site. By gating on FSC$^{high}$CD3$^-$CD19$^-$CD11c$^+$I-A$_b^+$ cells, we found that tumor tissues were infiltrated by large numbers of CD11b$^+$ DC that were negative for the Langerhans cell marker EpCAM, plasmacytoid DC marker PDCA-1, resident LN/spleen DC marker CD8α, and myeloid DC marker CD4 (Figure 2A). Additionally, the TIDC did not express high levels of GR-1, a marker commonly associated with myeloid suppressor cells (40). This TIDC phenotype closely resembled that of normal dermal DC in the skin, as well as some of the DC found in the skin DLN that are thought to be the recent dermal DC migrants (Figure 2A). Interestingly, the number of TIDC was about 100-fold higher than the number of dermal DC in the skin site. When normalized based on the volume of tissue sampled, TIDC density surpassed that of the dermal DC in the skin by about 10-fold (Figure. 2C). There were no differences in total number and density of CD11b+ DC in skin vs. tumor DLN (Figure 2B,C), even though tumor DLN were often enlarged. Fluorescence microscopic examination of frozen tumor samples revealed that tumors were infiltrated by CD11b$^+$ TIDC throughout the entirety of the tissue, and in some parts, including peripheral edges of the tumor, exhibited areas of high tissue infiltration (Figure 2D).

To further characterize TIDC phenotype, we examined overall DC activation status by looking at MHC-II and costimulatory molecule expression. TIDC expressed intermediate levels of MHC-II, as compared to bulk skin LN CD11b$^+$ DC (Figure 2E). Interestingly, both MHC-II$^{high}$ and the majority of MHC-II$^{low}$ TIDC displayed high levels of CD86 and CD80 surface expression. However, CD40 expression was overall lower in comparison to MHC-II$^{high}$ LN DC (Figure 2E). In addition, TIDC did not produce significant levels of IL-12, suggesting that they were not fully activated (data not shown). In contrast to the partially activated phenotype of the TIDC, normal dermal DC displayed a fully immature phenotype (data not shown), consistent with the notion that DC migrate out of normal peripheral tissues upon maturation. Taken as a whole, these results indicated that tumors were well infiltrated by large numbers of TIDC that displayed normal interstitial DC markers and exhibited a partially activated phenotype.

### TIDC exhibit marked differences in migration to DLN compared to dermal DC

The inability to find many GFP$^+$ DC in tumor DLN (Figure 1A), despite large numbers of DC in the tumor, could have been due to poor ability of TIDC to migrate to DLN over the times we examined. Because GFP fluorescence will decrease over time due to proteolysis, we utilized indigestible, 1μm-sized red fluospheres to compare the ability of dermal DC and TIDC to migrate from the peripheral injection site to the DLN. Injection of $5\times10^8$ beads either s.c. or i.t. resulted in phagocytosis of the beads at the respective sites by both dermal DC and TIDC within 4hr (Figure 3A), and there was at least a 10-fold greater number of bead positive DC in the tumor compared to the dermis (Figure 3B). This is not surprising considering that the total number of TIDC is much greater than the skin surrounding the s.c. injection site (Figure 2B). While the total number of bead$^+$ dermal DC in the skin declined over time, the overall number of bead$^+$ TIDC remained relatively unchanged, resulting in even greater differences in total numbers of bead$^+$ DC (Figure 3B). To examine the kinetics of DC migration to the DLN, we gated on FSC$^{high}$CD3$^-$CD19$^-$CD11c$^+$CD11b$^+$I-A$_b^{+/high}$ cell subset to reduce the background due to bead uptake by resident LN DC, since all dermal and TIDC are CD11b$^+$ and are of a mature phenotype upon migration to DLN (26, 35). Even though the numbers of DC were drastically different at the injection sites (Figure 3B), the total numbers found in the tumor and

skin DLN were virtually identical, as were the rates of accumulation (Figure 3C). These data suggested that on a population level, TIDC were defective in migrating to DLN, consistent with the fact that the total numbers of $CD11b^+$ DC in skin and tumor DLN were equivalent, even though tumor DLN were draining a site containing large numbers of DC (Figure 2B). Even though the TIDC were poor at migrating to DLN as compared to dermal DC, the total number of migrants found in DLN was comparable, suggesting that DC migration capacity could not fully explain the low Ag levels and MHC-II presentation in tumor DLN DC.

## TIDC are poor at Ag uptake compared to dermal DC

Following injection of EαGFP, the overall intracellular GFP mean fluorescence intensity (MFI) was substantially lower in tumor DLN DC compared with the skin DLN DC (Figure 1B), suggesting that TIDC may take up less protein than dermal DC. To examine this, we performed a kinetic comparison of EαGFP uptake by dermal DC in the skin and TIDC inside the tumor. While both dermal DC and TIDC quickly took up EαGFP protein, dermal DC were vastly superior to TIDC in overall level of uptake at all time points (Figure 4A–C). Kinetic comparison revealed that even though the GFP MFI was substantially lower for TIDC, the overall percent of $GFP^+$ TIDC at the peak of uptake (~4hr) was not that dissimilar from dermal DC at the peak of uptake (~3hr) (Figure 4B). Since the intracellular GFP MFI levels were frequently ~10 fold lower in TIDC than in dermal DC, we tested whether increasing the EαGFP inoculation dose by 10 fold (500μg) would rescue Ag uptake in TIDC. Interestingly, while the overall TIDC GFP MFI levels rose substantially to the levels seen in dermal DC after a 50μg injection, TIDC Ag uptake remained vastly inferior to dermal DC for the 500μg dose (Figure 4A,D).

Considering that the total number of DC was much greater inside the tumor as compared to the dermal site (Figure 2B), it was possible that TIDC were simply competing more for the low levels of available soluble protein. In addition, s.c. and i.t. injections deliver proteins into distinctive sites with different microenvironments and tissue volumes, thus making it possible that DC extrinsic differences account for the differences in uptake. To test whether the protein uptake differences seen were due to cell intrinsic or extrinsic mechanisms, we purified dermal DC and TIDC from the tissues and plated the cells *ex vivo* with different concentrations of EαGFP for 45 minutes at 37ºC to allow uptake of the soluble protein with cells under similar conditions. However, even under these conditions, the TIDC were inferior to dermal DC in their ability to take up protein to a similar extent as observed *in vivo* (Figure 4E). These profound Ag uptake differences by TIDC were observed in all of the tested tumor systems (Figure 4F). These results showed that while both normal dermal DC and TIDC mediated maximal protein uptake within several hours of protein delivery, dermal DC were intrinsically superior to TIDC in the overall uptake capacity.

## Dermal DC and TIDC exhibit similar protein degradation kinetics

It has been recently shown that enhanced lysosomal protein degradation by DC can lead to reduced levels of intracellular protein both in the periphery and in DLN, and cause a reduction of MHC-II presentation to CD4 T cells (34). Thus, in addition to reduced uptake, enhanced degradative capacity in TIDC could potentially contribute to the lower levels of EαGFP protein observed in the DLN. To examine protein degradation we determined the intracellular protein remaining over time as a percent of the level at the peak of uptake (3hr for dermal DC; 4hr for TIDC). The rates of loss of fluorescence for dermal DC and TIDC were essentially identical, suggesting that the speed of protein processing was similar in both cell types (Figure 5A). Interestingly, we found that the overall levels of intracellular EαGFP quickly stabilized following an initial phase of degradation in both dermal DC and TIDC, suggesting that some of the protein may be entering into the nondegradative intracellular vesicular compartment (41). Considering that the levels of intracellular protein were much higher in dermal DC than in TIDC (Figure 4C), we compared the decrease in GFP MFI over 24hr in dermal DC and

TIDC in a situation where the levels of intracellular EαGFP were equivalent by injecting 50μg s.c. for dermal DC and 500μg i.t. for TIDC. Here too, the rate of decrease in fluorescence was identical for dermal DC and TIDC (Figure 5B), again indicating that the overall rates of protein degradation were similar for these cells and independent of intracellular protein concentration.

To confirm these results in an EαGFP-independent assay, we utilized a fluorogenic DQ Ovalbumin protein (DQ-OVA). DQ-OVA is heavily conjugated to BODIPY fluorescent dyes that reach autoquenching levels, thus only becoming fluorescent after intracellular proteolytic degradation and physical separation of the OVA peptides. We hypothesized that if the decreased intracellular protein content and MHC-II presentation in tumor DLN DC (Figure 1A) is solely due to enhanced rates of protein degradation by TIDC, then we would observe greater intracellular FL-1 fluorescence levels in TIDC DLN migrants compared to s.c. dermal DC migrants after DQ-OVA inoculation. In contrast, we observed a reduced percentage of FL-$1^+$ DC, and more importantly much lower FL-1 MFI of FL-$1^+$CD$11b^+$ DC in the tumor DLN compared to skin DLN (Figure 5C). These results were consistent with TIDC picking up lower amounts of DQ-OVA protein at the tumor site before migrating to the DLN, thus resulting in lower fluorescence levels following DQ-OVA degradation. Together these results strongly argued that dermal DC and TIDC have comparable protein degradation kinetics, and that the primary defect in TIDC is the reduced ability to take up proteins.

### TIDC and dermal DC exhibit similar intrinsic MHC-II presentation capacity

The above results demonstrate that TIDC are less efficient than dermal DC in taking up protein Ag. It was also possible that a reduced ability to process the protein and form I-$A_b$-E$\alpha^{52–68}$ complexes might contribute to the reduced levels of MHC-II-peptide complexes on migratory TIDC compared to dermal DC in the DLN (Figure 1A). To examine this, we compared the ability of these subsets to present EαGFP on MHC-II at the peripheral site prior to migration. The overall percent of both TIDC and dermal DC presenting I-$A_b$-E$\alpha^{52–68}$ complexes was relatively low (Figure 6A), even though a majority of cells had taken up EαGFP protein (Figure 4A). $GFP^+$ TIDC exhibited a lower percentage and MFI of $YAe^+$ cells than dermal DC at the 50μg dose of injected protein (Figure 6A,B), but this difference was not found when a 500μg dose of protein was injected. Considering that dermal DC took up more soluble protein than TIDC, and that Ag presentation of I-$A_b$-E$\alpha^{52–68}$ complexes appeared to positively correlate with the amount of intracellular protein (Figure 4A), we normalized the protein uptake of the DC populations by creating a series of gates of increasing GFP MFI (Figure 6C). This allowed us to compare presentation of I-$A_b$-E$\alpha^{52–68}$ complexes by dermal DC and TIDC that had taken up similar amounts of EαGFP. This analysis revealed that both dermal DC and TIDC were indistinguishable in their presentation capacity, since both the percent of $YAe^+$ cells and the YAe MFI increased comparably with increasing levels of intracellular EαGFP for both cell types (Figure 6D and 6E). These results argued that the observed deficiency in TIDC MHC-II presentation on the population level was not due to an intrinsic inability of the cells to process Ag, but due to the defective uptake that resulted in lower intracellular levels of EαGFP available for processing. These results also demonstrated that peripheral MHC-II presentation in both normal skin and tumor peripheral sites requires fairly robust Ag uptake, and that the level of MHC-II-peptide complex formation appears to directly correlate with amount of ingested protein.

Even though DC are thought to be the predominant Ag presenting cell population, macrophages can also process proteins for MHC-II presentation, albeit at much lower levels (34). We found that tumors contained a large population of tumor infiltrating CD$11b^+$CD$11c^-$ macrophages (Figure 7A). Interestingly macrophages found in the dermis and the tumor took up similar levels of EαGFP as their DC counterparts, indicating that inhibition of Ag uptake by the tumor microenvironment extended to multiple immune cell types (Figure 7B). Importantly,

macrophages in both the dermis and the tumor were significantly worse than DC in processing soluble proteins for MHC-II presentation (Figure 7C), suggesting that DC may be the dominant Ag presenting cell in both DLN and in peripheral skin and tumor sites, and that neither TIDC nor tumor infiltrating macrophages efficiently present soluble proteins (34).

### TIDC are poor at presenting proteins to effector CD4 T Cells in vivo

We previously showed that DC in tumor DLN were not presenting Ag to naïve CD4 T cells, which in turn prevented the potential for indirect helper effects as well as for direct anti-tumor activity (35). These results suggested that the ignorant status of tumor-specific CD4 T cells might allow for effective therapeutic immunization of the naïve CD4 cell pool even after initiation of robust tumor growth. However, the poor ability of TIDC to present soluble proteins on MHC-II (Figure 6A) raised the possibility that even if effector CD4 T cells did traffic to the tumor site post immunization, they would not be restimulated to elicit anti-tumor effects. Consistent with this hypothesis, TIDC purified from B16.OVA melanoma tumors were incapable of activating OVA-specific OT-II CD4 T cells directly *ex vivo* (*35*. To test whether TIDC could function as Ag presenting cells in the tumor *in vivo*, we adoptively transferred naïve OT-I and OT-II T cells (OVA-specific CD8 and CD4 T cells, respectively) into C57BL/6 mice that were then s.c. challenged with B16.F10 and B16.OVA tumor cells injected into contralateral sides (Figure 8A). Injection of both B16.F10 and B16.OVA into the same animals allowed for discrimination of T cell tumor infiltration, accumulation, and sensing of presented OVA protein in an Ag-specific manner within the same host. Some of the animals were then immunized with OVA protein and LPS adjuvant i.v. on day 6 of tumor growth to stimulate robust activation and expansion of effector OT-I and OT-II T cells. Without immunization, the total number of OT-I T cells in the spleen and the two tumor sites combined only increased ~3 fold after 12 days of tumor growth, compared to tumor-free animals, consistent with the previous findings of tolerogenic CD8 T cell activation (35). As previously shown, OT-II T cells remained naïve (ignorant), did not undergo expansion, and did not traffic to the tumor site without immunization (Figure 8B and data not shown). OVA/LPS immunization induced robust expansion of both OT-I and OT-II T cells in the examined tissues, with OT-I T cells totally expanding about 4 fold more than OT-II T cells (Figure 8B). Examination of the T cell tissue distribution revealed a large prevalence of OT-I T cells in the B16.OVA tumor, with relatively low numbers of cells in the spleen and the B16.F10 tumor (Figure 8C). In contrast, OT-II T cells largely remained in the spleen, did not infiltrate either tumor in large numbers, and did not preferentially accumulate in an Ag-dependent manner in the B16.OVA tumor. This resulted in greater than a 2,500-fold difference in OT-I vs. OT-II cell numbers in the B16.OVA tumor site (Figure 8C). Interestingly, both OT-I and the small number of OT-II T cells in the B16.OVA tumor upregulated CD69 expression. This suggested that a low level of MHC-II presentation may occur within the tumor, but be insufficient to promote CD4 T cell accumulation and/or division (Figure 8D). In agreement with low CD4 T cell accumulation and hence marginal anti-tumor function, we observed minimal effects on tumor growth after immunization, which was to some degree surprising considering the degree of CD8 T cell infiltration (data not shown). Together these results indicated that while activated CD8 T cells could infiltrate the tumor in great numbers and robustly sense MHC-I-peptide complexes, effector CD4 T cells were poor at overall migration and Ag-specific retention at the tumor site, likely as a result of defective Ag uptake and presentation on MHC-II by TIDC.

### TLR mediated TIDC maturation does not rescue *Ag* uptake and DLN MHC-II presentation

Toll like receptor (TLR) stimulation has been shown to induce peripheral DC maturation and to cause enhanced human and murine TIDC function and cytokine secretion *ex vivo* (38,39). Additionally, DC maturation has been observed to transiently increase Ag uptake *in vitro* and induce migration of DC from the peripheral tissues to the DLN *in vivo* (25,42). We therefore tested whether TLR induced TIDC activation could rescue Ag uptake in the tumor and

presentation in the DLN by co-injecting EαGFP protein with TLR9 ligand CpG, TLR3 ligand polyI:C, or TLR4 ligand LPS. As expected, all TLR ligands induced a robust increase in MHC-II presentation in skin DLN after s.c. inoculation into non-tumor bearing animals (Figures 9A). In contrast, i.t. administration of TLR ligand induced marginal effects on Ag presentation in tumor DLN, consistently showing significantly lower percentages of $GFP^+YAe^+$ DC as compared to skin DLN (Figure 9A). In addition, while the overall intracellular GFP levels were increased in migratory dermal DC in skin DLN, there was no effect on GFP levels in the $GFP^+$ DC found in tumor DLN (Figure 9B). Importantly, peripheral tissue Ag uptake by either dermal DC or TIDC was unaltered in response to TLR stimulation (Figure 9C). We consistently observed enhanced maturation of peripheral dermal DC in response to CpG at 3hr and to polyI:C and LPS at 24hr post injection, and clear TIDC maturation in response to CpG and LPS TLR ligands, indicating that TIDC were at least partially responsive to TLR stimulation (Figure 9D, and data not shown). Additionally, most DLN DC exhibited a mature phenotype 24hr post TLR injection, demonstrating the effectiveness of immunization (data not shown). These data suggested that increased GFP MFI levels observed in dermal DC migrants in skin DLN after TLR ligand injection was not primarily due to enhanced peripheral protein uptake, but potentially due to increased DC migration speed and/or decreased degradation rates. In agreement with this, we observed a decrease in the rate of protein degradation in peripheral dermal DC after polyI:C administration (data not shown). Additionally, while not being able to measure TLR-induced dermal DC migration, we observed an enhancement of TIDC migration to DLN post CpG treatment in experiments using fluorescent microspheres (data not shown).

Interestingly, in several experiments we observed a mild but significant enhancement of TIDC Ag presentation 24hrs after CpG administration, even though no significant increase was seen for dermal DC (Figure 9E). However, a CpG immunization trial failed to induce naïve CD4 T cell priming in the DLN and i.t. effector CD4 T cell accumulation, suggesting that the major limitation for optimal DC function continued to be poor tumor-Ag uptake and not overall MHC-II processing (data not shown). These results suggested that even though the tested TLR ligands could cause enhanced maturation and migration to DLN in dermal and TIDC , they did not significantly enhance *in vivo* peripheral tissue Ag uptake and therefore had minimal effects on peripheral MHC-II presentation.

## Discussion

Adaptive immune responses are initiated by the presentation of peptides from foreign proteins on MHC molecules by DC in the 2º lymphoid sites. We have previously observed that CD8 T cell responses to cytoplasmic and secreted tumor-Ag can be robust but result in overall tolerance induction (35). In contrast, CD4 T cells remain ignorant throughout disease progression, due to defective MHC-II presentation of tumor-derived proteins on DLN DC. We have now examined the basis for this defective MHC-II presentation in several s.c. cancer models and on two murine backgrounds. We found that tumors are infiltrated by large numbers $CD11b^+$ DC, a large fraction of which have a partially activated phenotype. In comparison to normal dermal DC, these TIDC are very inefficient at taking up soluble proteins, but are comparable in the relative rates of protein degradation and formation of MHC-II-peptide complexes. While TIDC exhibit a partial block in migration to the DLN, these data show that the inability to present sufficient Ag to activate naïve CD4 T cells in the DLN, or stimulate effector CD4 T cells within the tumor appears to result primarily from the limited capacity of TIDC to internalize protein Ag.

Interestingly, the contrasting responses of CD8 and CD4 T cells to the same tumor-secreted protein suggest that MHC-I and MHC-II presentation in the DLN is physically uncoupled and is differentially regulated. In agreement with this notion, we found that while the LN resident

CD8α$^+$ DC were efficient at cross-presenting tumor-derived proteins to CD8 T cells, only the activated/migratory CD11b$^+$ DC had any detectable MHC-II-peptide complexes (35). These findings suggest a model where the DLN receives tumor-derived lymph fluid carrying cell debris along with various tumor proteins and cell membranes, which then gets efficiently taken up by immature CD8α$^+$ DC and selectively directed towards MHC-I processing (43). At the same time, TIDC are poor at protein uptake and to some degree migration, and are thus unable to function as professional APC in the DLN for initiating CD4 T cell priming. The proposed scenario for anti-tumor responses is similar to one described by Jenkins and colleagues for soluble protein immunization, where Ag presentation to CD4 T cells in the DLN occurs via both resident and migratory DC, with the exception that in the tumor model the draining proteins are cell-associated and hence are targeted to MHC-I presentation and migratory DC are defective at Ag uptake and therefore MHC-II presentation (26). However, it is entirely plausible that in addition to TIDC defects, resident DLN DC have defective MHC-II presentation machinery and contribute to CD4 T cell ignorance. Elucidating these non-mutually exclusive mechanisms behind the apparent MHC-I/II presentation paradox will require further study.

Microscopic examination revealed that TIDC heavily infiltrated the peripheral and inner parts of the tumor tissues with some indication of infiltration-rich regions. Phenotypic examination of TIDC showed that they were largely indistinguishable from normal interstitial dermal DC, which is in agreement with other data that has described a large prevalence of CD11b$^+$ DC infiltrating various murine tumors (36,44). Interestingly, in contrast to the immature peripheral dermal DC, TIDC expressed intermediate to high MHC-II and co-stimulatory levels, and low levels of intracellular IL-12. These results suggest that TIDC undergo a partial maturation program, possibly through experiencing inflammatory cytokines, such as TNFα, at the tumor site (45). It has been shown that DC maturation decreases phagocytosis and prevents uptake and presentation of proteins on MHC (42,46). It is thus possible that the partial activation state of TIDC is at least in part responsible for causing poor Ag uptake and MHC-II presentation. This is consistent with the fact that the immature dermal DC were efficient at Ag uptake, which allowed them to maintain high levels of available intracellular protein after maturation and migration to the DLN. These high intracellular protein levels appeared to directly correlate with the amount of detectable surface MHC-II-peptide complexes in both the periphery and the DLN, suggesting that efficient Ag acquisition is required for optimal MHC-II presentation. We found that TLR ligand co-administration caused an increase in maturation and migration in both dermal DC and TIDC and greatly enhanced Ag presentation in skin DLN. This treatment however failed to alter peripheral Ag uptake in both subsets. While it has been shown that DC undergo a transient increase in Ag phagocytosis post TLR induced maturation *in vitro*, our results argue that Ag acquisition *in vivo* occurs relatively rapidly and independently of simultaneous TLR signaling (42). Interestingly, after the initial uptake and degradative phase, dermal DC appeared to store the protein at fairly stable levels, suggesting that the some of the soluble protein can enter the nondegradative intracellular vesicular compartment that has been described to play a role in Ag transfer to B cells (41,47). It is also possible that limiting Ag processing for MHC-II presentation in the periphery could be important for reducing tissue inflammation and destruction during the effector CD4 T cell response. It is important to note that the observed DC Ag handling characteristics describe responses to soluble proteins, which are likely to be different from bacterial or viral infections.

It has been recently shown that i.t. T cell infiltration and accumulation directly correlates with therapeutic efficacy (48). In our hands, poor Ag uptake and presentation by TIDC not only precluded the initial priming of CD4 T cells in DLN, but also appeared to prevent effector CD4 T cell accumulation at the tumor site and correlated with a lack of tumor regression (35). Even i.t.administration of CpG, which was observed to partially enhance MHC-II presentation but not Ag uptake, was incapable of rescuing effector CD4 T cell accumulation. Interestingly, we

also observed differences between Ag-nonspecific CD8 and CD4 T cell tumor infiltration, with CD8 T cells being much better than CD4 T cells at infiltrating the neoplastic tissues. In agreement, we have previously observed that endogenous CD8 T cells vastly outnumbered CD4 T cells inside the tumor (35). While we initially attributed these results to reduced initial priming of endogenous CD4 T cells in tumor DLN, it is possible that both priming and ability to infiltrate the tumor is defective in the CD4 T cell population. While defective tumor infiltration by T cells has been previously observed and attributed to a lack of integrin expression on the tumor endothelium, the disparity between CD4 and CD8 T cell infiltration observed in our model suggests that differences in various adhesion molecules exist directly on CD4 and CD8 effector T cells (48,49).

Interestingly, TIDC were efficient at infiltrating and accumulating to great numbers inside the tumor tissue, suggesting that this immune cell subset carries the appropriate adhesion molecules for proper tumor infiltration. On the other hand, TIDC were relatively poor at migrating to the DLN, suggesting that TIDC do not possess the necessary surface molecules to mediate exit or to guide them into the DLN. However, it is also possible that disease-associated tissue microenvironment is simply not permissive for TIDC migration after initial infiltration. Further characterization of integrin and adhesion molecule expression and function on tumor endothelium, effector CD4 and CD8 T cells, and TIDC is necessary to understand the requirements for immune cell trafficking into and out of neoplastic tissues.

While poor TIDC migration likely contributed to CD4 T cell ignorance, it is clear that defective Ag acquisition by TIDC served as the major limiting step in both initiation and facilitation of anti-tumor CD4 T cell responses. This defect can be attributed to several different non-mutually exclusive mechanisms. In addition to partial maturation, improper TIDC differentiation due to a lack of appropriate growth factors in the tumor microenvironment can cause poor Ag uptake. It is also possible that inhibitory factors present in the tumor may cause specific deregulation of TIDC function (50,51). While TGFβ and IL-10 have been described to negatively modulate anti-tumor immune responses, we did not observe enhancement of Ag uptake by TIDC or initiation of CD4 T cell priming in DLN after TGFβ antibody blockade or in IL-10 deficient animals, respectively (unpublished observations). However, it is possible that several suppressive factors act to inhibiting TIDC functional competence and/or differentiation, and neutralization of all of them is necessary for restoration of TIDC function (50,51). Additionally, nutrient starvation is likely to occur at the tumor site and has been previously shown to induce autophagy and reduce soluble Ag capture, thus specifically decreasing presentation of peripheral proteins and enhancing presentation of self-proteins on MHC-II (52). Interestingly, we observed that tumor infiltrating macrophages also took up lower levels of Ag as compared to their normal skin counterparts. While clearly not being as efficient at Ag processing for MHC-II presentation as DC, these results suggest that inhibition of Ag uptake by the tumor microenvironment is a global phenomenon that extends to multiple immune cell subsets. Understanding the mechanisms behind defective Ag acquisition as well as immune cell migration should allow for better understanding of clinical data from various immunotherapy trials and more importantly for enhancing design of future therapeutic regimens.

## Nonstandard Abbreviations

DLN, draining lymph node; i.t., intratumoral; Mϕ, macrophage; TIDC, tumor infiltrating DC.

## Acknowledgements

Grant Support: This research was supported by National Institutes of Health grants AI34824 (M.F.M.), CA82596 (M.F.M.), and NCI 2 T32 CA009138-31 (M.Y.G.).

We would like to thank Dr. Stephen C. Jameson, Dr. Marc K. Jenkins, Dr. Christopher A. Pennell, Dr. Dan Kaplan, and Kerry A. Casey for critical discussion. The authors have no conflicting financial interests.

## References

1. Zitvogel L, Tesniere A, Kroemer G. Cancer despite immunosurveillance: immunoselection and immunosubversion. Nat. Rev. Immunol 2006;6:715–727. [PubMed: 16977338]
2. Shrikant P, Khoruts A, Mescher MF. CTLA-4 blockade reverses CD8+ T cell tolerance to tumor by a CD4+ T cell- and IL-2-dependent mechanism. Immunity 1999;11:483–493. [PubMed: 10549630]
3. Antony PA, Piccirillo CA, Akpinarli A, Finkelstein SE, Speiss PJ, Surman DR, Palmer DC, Chan CC, Klebanoff CA, Overwijk WW, Rosenberg SA, Restifo NP. CD8+ T cell immunity against a tumor/self-antigen is augmented by CD4+ T helper cells and hindered by naturally occurring T regulatory cells. J. Immunol 2005;174:2591–2601. [PubMed: 15728465]
4. Perez-Diez A, Joncker NT, Choi K, Chan WF, Anderson CC, Lantz O, Matzinger P. CD4 cells can be more efficient at tumor rejection than CD8 cells. Blood 2007;109:5346–5354. [PubMed: 17327412]
5. Muranski P, Boni A, Antony PA, Cassard L, Irvine KR, Kaiser A, Paulos CM, Palmer DC, Touloukian CE, Ptak K, Gattinoni L, Wrzesinski C, Hinrichs CS, Kerstann KW, Feigenbaum L, Chan CC, Restifo NP. Tumor-specific Th17-polarized cells eradicate large established melanoma. Blood 2008;112:362–373. [PubMed: 18354038]
6. Wong SB, Bos R, Sherman LA. Tumor-specific CD4+ T cells render the tumor environment permissive for infiltration by low-avidity CD8+ T cells. J. Immunol 2008;180:3122–3131. [PubMed: 18292535]
7. Miga AJ, Masters SR, Durell BG, Gonzalez M, Jenkins MK, Maliszewski C, Kikutani H, Wade WF, Noelle RJ. Dendritic cell longevity and T cell persistence is controlled by CD154-CD40 interactions. Eur. J. Immunol 2001;31:959–965. [PubMed: 11241301]
8. Mescher MF, Curtsinger JM, Agarwal P, Casey KA, Gerner M, Hammerbeck CD, Popescu F, Xiao Z. Signals required for programming effector and memory development by CD8+ T cells. Immunol. Rev 2006;211:81–92. [PubMed: 16824119]
9. Delamarre L, Holcombe H, Mellman I. Presentation of exogenous antigens on major histocompatibility complex (MHC) class I and MHC class II molecules is differentially regulated during dendritic cell maturation. J. Exp. Med 2003;198:111–122. [PubMed: 12835477]
10. Mueller SN, Jones CM, Stock AT, Suter M, Heath WR, Carbone FR. CD4+ T cells can protect APC from CTL-mediated elimination. J. Immunol 2006;176:7379–7384. [PubMed: 16751382]
11. Cella M, Scheidegger D, Palmer-Lehmann K, Lane P, Lanzavecchia A, Alber G. Ligation of CD40 on dendritic cells triggers production of high levels of interleukin-12 and enhances T cell stimulatory capacity: T-T help via APC activation. J. Exp. Med 1996;184:747–752. [PubMed: 8760829]
12. Hochweller K, Anderton SM. Kinetics of costimulatory molecule expression by T cells and dendritic cells during the induction of tolerance versus immunity in vivo. Eur. J. Immunol 2005;35:1086–1096. [PubMed: 15756642]
13. Castellino F, Huang AY, Altan-Bonnet G, Stoll S, Scheinecker C, Germain RN. Chemokines enhance immunity by guiding naive CD8+ T cells to sites of CD4+ T cell-dendritic cell interaction. Nature 2006;440:890–895. [PubMed: 16612374]
14. Tham EL, Shrikant P, Mescher MF. Activation-induced nonresponsiveness: a Th-dependent regulatory checkpoint in the CTL response. J. Immunol 2002;168:1190–1197. [PubMed: 11801654]
15. Williams MA, Tyznik AJ, Bevan MJ. Interleukin-2 signals during priming are required for secondary expansion of CD8+ memory T cells. Nature 2006;441:890–893. [PubMed: 16778891]
16. van Mierlo GJ, Boonman ZF, Dumortier HM, den Boer AT, Fransen MF, Nouta J, van der Voort EI, Offringa R, Toes RE, Melief CJ. Activation of dendritic cells that cross-present tumor-derived antigen licenses CD8+ CTL to cause tumor eradication. J. Immunol 2004;173:6753–6759. [PubMed: 15557168]
17. Sun JC, Williams MA, Bevan MJ. CD4+ T cells are required for the maintenance, not programming, of memory CD8+ T cells after acute infection. Nat. Immunol 2004;5:927–933. [PubMed: 15300249]
18. Shedlock DJ, Shen H. Requirement for CD4 T cell help in generating functional CD8 T cell memory. Science 2003;300:337–339. [PubMed: 12690201]

19. Smith CM, Wilson NS, Waithman J, Villadangos JA, Carbone FR, Heath WR, Belz GT. Cognate CD4(+) T cell licensing of dendritic cells in CD8(+) T cell immunity. Nat. Immunol 2004;5:1143–1148. [PubMed: 15475958]
20. Wang JC, Livingstone AM. Cutting edge: CD4+ T cell help can be essential for primary CD8+ T cell responses in vivo. J. Immunol 2003;171:6339–6343. [PubMed: 14662830]
21. Curtsinger JM, Lins DC, Mescher MF. Signal 3 determines tolerance versus full activation of naive CD8 T cells: dissociating proliferation and development of effector function. J. Exp. Med 2003;197:1141–1151. [PubMed: 12732656]
22. Hollenbaugh JA, Dutton RW. IFN-gamma regulates donor CD8 T cell expansion, migration, and leads to apoptosis of cells of a solid tumor. J. Immunol 2006;177:3004–3011. [PubMed: 16920936]
23. Dunn GP, Koebel CM, Schreiber RD. Interferons, immunity and cancer immunoediting. Nat. Rev. Immunol 2006;6:836–848. [PubMed: 17063185]
24. Haring JS, Badovinac VP, Harty JT. Inflaming the CD8+ T cell response. Immunity 2006;25:19–29. [PubMed: 16860754]
25. Villadangos JA, Schnorrer P. Intrinsic and cooperative antigen-presenting functions of dendritic-cell subsets in vivo. Nat. Rev. Immunol 2007;7:543–555. [PubMed: 17589544]
26. Itano AA, McSorley SJ, Reinhardt RL, Ehst BD, Ingulli E, Rudensky AY, Jenkins MK. Distinct dendritic cell populations sequentially present antigen to CD4 T cells and stimulate different aspects of cell-mediated immunity. Immunity 2003;19:47–57. [PubMed: 12871638]
27. Scheinecker C, McHugh R, Shevach EM, Germain RN. Constitutive presentation of a natural tissue autoantigen exclusively by dendritic cells in the draining lymph node. J. Exp. Med 2002;196:1079–1090. [PubMed: 12391019]
28. Leon B, Lopez-Bravo M, Ardavin C. Monocyte-derived dendritic cells formed at the infection site control the induction of protective T helper 1 responses against Leishmania. Immunity 2007;26:519–531. [PubMed: 17412618]
29. Celli S, Garcia Z, Bousso P. CD4 T cells integrate signals delivered during successive DC encounters in vivo. J. Exp. Med 2005;202:1271–1278. [PubMed: 16275764]
30. Mount AM, Smith CM, Kupresanin F, Stoermer K, Heath WR, Belz GT. Multiple dendritic cell populations activate CD4+ T cells after viral stimulation. PLoS ONE 2008;3:e1691. [PubMed: 18301768]
31. Dudziak D, Kamphorst AO, Heidkamp GF, Buchholz VR, Trumpfheller C, Yamazaki S, Cheong C, Liu K, Lee HW, Park CG, Steinman RM, Nussenzweig MC. Differential antigen processing by dendritic cell subsets in vivo. Science 2007;315:107–111. [PubMed: 17204652]
32. Hochrein H, Shortman K, Vremec D, Scott B, Hertzog P, O'Keeffe M. Differential production of IL-12, IFN-alpha, and IFN-gamma by mouse dendritic cell subsets. J. Immunol 2001;166:5448–5455. [PubMed: 11313382]
33. Reinhardt RL, Bullard DC, Weaver CT, Jenkins MK. Preferential accumulation of antigen-specific effector CD4 T cells at an antigen injection site involves CD62E-dependent migration but not local proliferation. J. Exp. Med 2003;197:751–762. [PubMed: 12629067]
34. Delamarre L, Pack M, Chang H, Mellman I, Trombetta ES. Differential lysosomal proteolysis in antigen-presenting cells determines antigen fate. Science 2005;307:1630–1634. [PubMed: 15761154]
35. Gerner MY, Casey KA, Mescher MF. Defective MHC class II presentation by dendritic cells limits CD4 T cell help for antitumor CD8 T cell responses. J. Immunol 2008;181:155–164. [PubMed: 18566380]
36. Stoitzner P, Green LK, Jung JY, Price KM, Atarea H, Kivell B, Ronchese F. Inefficient presentation of tumor-derived antigen by tumor-infiltrating dendritic cells. Cancer. Immunol. Immunother 2008;57:1665–1673. [PubMed: 18311487]
37. Preynat-Seauve O, Schuler P, Contassot E, Beermann F, Huard B, French LE. Tumor-infiltrating dendritic cells are potent antigen-presenting cells able to activate T cells and mediate tumor rejection. J Immunol 2006;176:61–67. [PubMed: 16365396]
38. Perrot I, Blanchard D, Freymond N, Isaac S, Guibert B, Pacheco Y, Lebecque S. Dendritic cells infiltrating human non-small cell lung cancer are blocked at immature stage. J Immunol 2007;178:2763–2769. [PubMed: 17312119]

39. Vicari AP, Chiodoni C, Vaure C, Ait-Yahia S, Dercamp C, Matsos F, Reynard O, Taverne C, Merle P, Colombo MP, O'Garra A, Trinchieri G, Caux C. Reversal of tumor-induced dendritic cell paralysis by CpG immunostimulatory oligonucleotide and anti-interleukin 10 receptor antibody. J. Exp. Med 2002;196:541–549. [PubMed: 12186845]
40. Gabrilovich D. Mechanisms and functional significance of tumour-induced dendritic-cell defects. Nat Rev Immunol 2004;4:941–952. [PubMed: 15573129]
41. Bergtold A, Desai DD, Gavhane A, Clynes R. Cell surface recycling of internalized antigen permits dendritic cell priming of B cells. Immunity 2005;23:503–514. [PubMed: 16286018]
42. West MA, Wallin RP, Matthews SP, Svensson HG, Zaru R, Ljunggren HG, Prescott AR, Watts C. Enhanced dendritic cell antigen capture via toll-like receptor-induced actin remodeling. Science 2004;305:1153–1157. [PubMed: 15326355]
43. Li M, Davey GM, Sutherland RM, Kurts C, Lew AM, Hirst C, Carbone FR, Heath WR. Cell-associated ovalbumin is cross-presented much more efficiently than soluble ovalbumin in vivo. J. Immunol 2001;166:6099–6103. [PubMed: 11342628]
44. Vicari AP, Chiodoni C, Vaure C, Ait-Yahia S, Dercamp C, Matsos F, Reynard O, Taverne C, Merle P, Colombo MP, O'Garra A, Trinchieri G, Caux C. Reversal of tumor-induced dendritic cell paralysis by CpG immunostimulatory oligonucleotide and anti-interleukin 10 receptor antibody. J. Exp. Med 2002;196:541–549. [PubMed: 12186845]
45. Lutz MB, Schuler G. Immature, semi-mature and fully mature dendritic cells: which signals induce tolerance or immunity? Trends Immunol 2002;23:445–449. [PubMed: 12200066]
46. Wilson NS, Behrens GM, Lundie RJ, Smith CM, Waithman J, Young L, Forehan SP, Mount A, Steptoe RJ, Shortman KD, de Koning-Ward TF, Belz GT, Carbone FR, Crabb BS, Heath WR, Villadangos JA. Systemic activation of dendritic cells by Toll-like receptor ligands or malaria infection impairs cross-presentation and antiviral immunity. Nat. Immunol 2006;7:165–172. [PubMed: 16415871]
47. Qi H, Egen JG, Huang AY, Germain RN. Extrafollicular activation of lymph node B cells by antigen-bearing dendritic cells. Science 2006;312:1672–1676. [PubMed: 16778060]
48. Quezada SA, Peggs KS, Simpson TR, Shen Y, Littman DR, Allison JP. Limited tumor infiltration by activated T effector cells restricts the therapeutic activity of regulatory T cell depletion against established melanoma. J. Exp. Med 2008;205:2125–2138. [PubMed: 18725522]
49. Buckanovich RJ, Facciabene A, Kim S, Benencia F, Sasaroli K, Balint D, Katsaros D, O'Brien-Jenkins A, Gimotty PA, Coukos G. Endothelin B receptor mediates the endothelial barrier to T cell homing to tumors and disables immune therapy. Nat. Med 2008;14:28–36. [PubMed: 18157142]
50. Gabrilovich D. Mechanisms and functional significance of tumour-induced dendritic-cell defects. Nat. Rev. Immunol 2004;4:941–952. [PubMed: 15573129]
51. Zou W. Immunosuppressive networks in the tumour environment and their therapeutic relevance. Nat. Rev. Cancer 2005;5:263–274. [PubMed: 15776005]
52. Dengjel J, Schoor O, Fischer R, Reich M, Kraus M, Muller M, Kreymborg K, Altenberend F, Brandenburg J, Kalbacher H, Brock R, Driessen C, Rammensee HG, Stevanovic S. Autophagy promotes MHC class II presentation of peptides from intracellular source proteins. Proc. Natl. Acad. Sci. U S A 2005;102:7922–7927. [PubMed: 15894616]

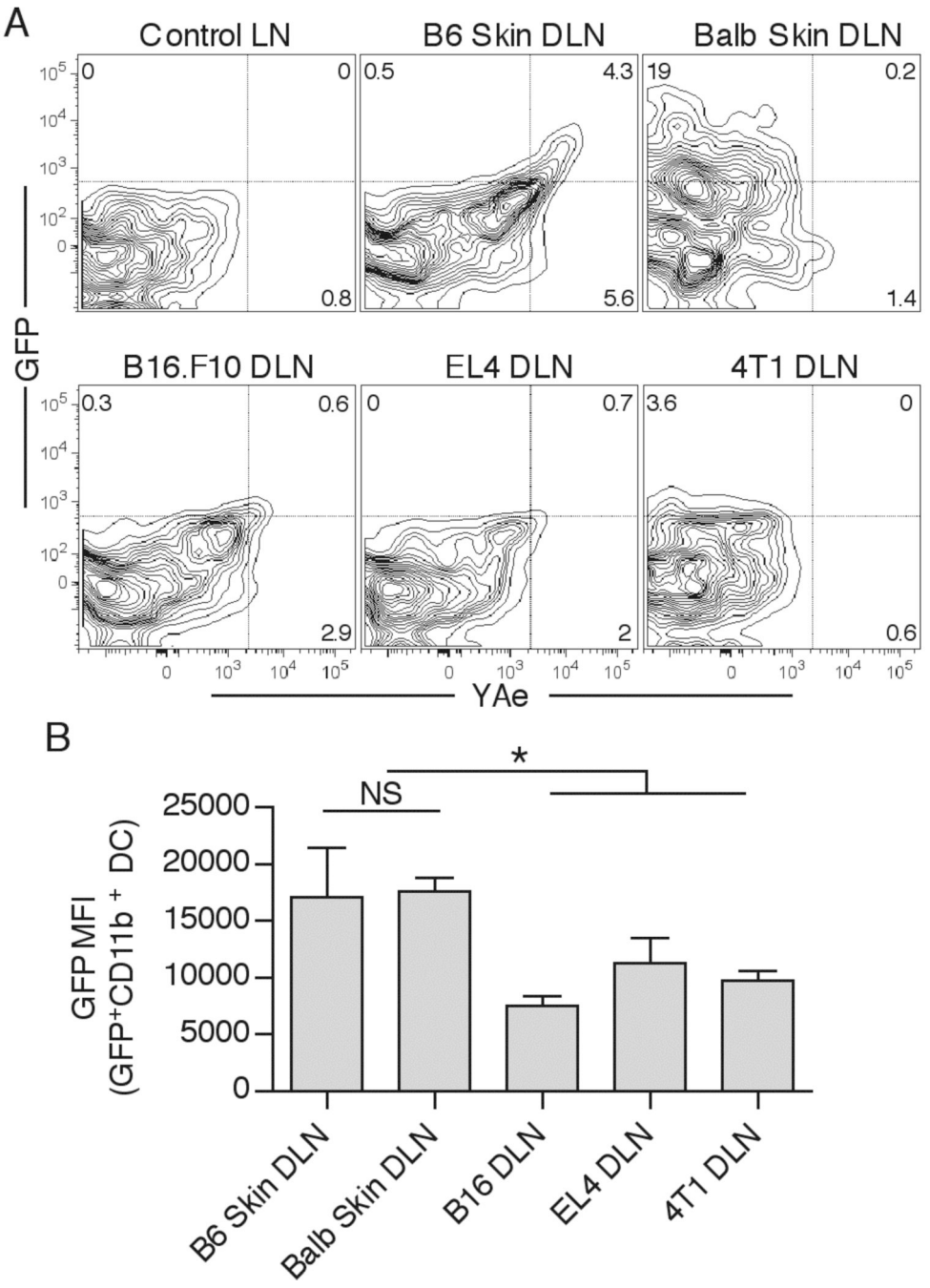


**Figure 1.**

Defective MHC-II Ag presentation in tumor DLN. Tumor-free C57Bl/6 and Balb/c mice, as well as day 10 B16.F10-bearing, day 8 EL4-bearing, and day 14 4T1-bearing animals were injected with 50μg EαGFP s.c. or i.t., respectively. 24hr later, $CD11b^+$ DC in DLN were examined for GFP fluorescence and YAe antibody staining (A). GFP mean fluorescence intensity (MFI) of $GFP^+CD11b^+$ DC in DLN samples was quantified (B). Numbers in the plots indicate percent cells in respective quadrant. Data are representative of at least two independent experiments.

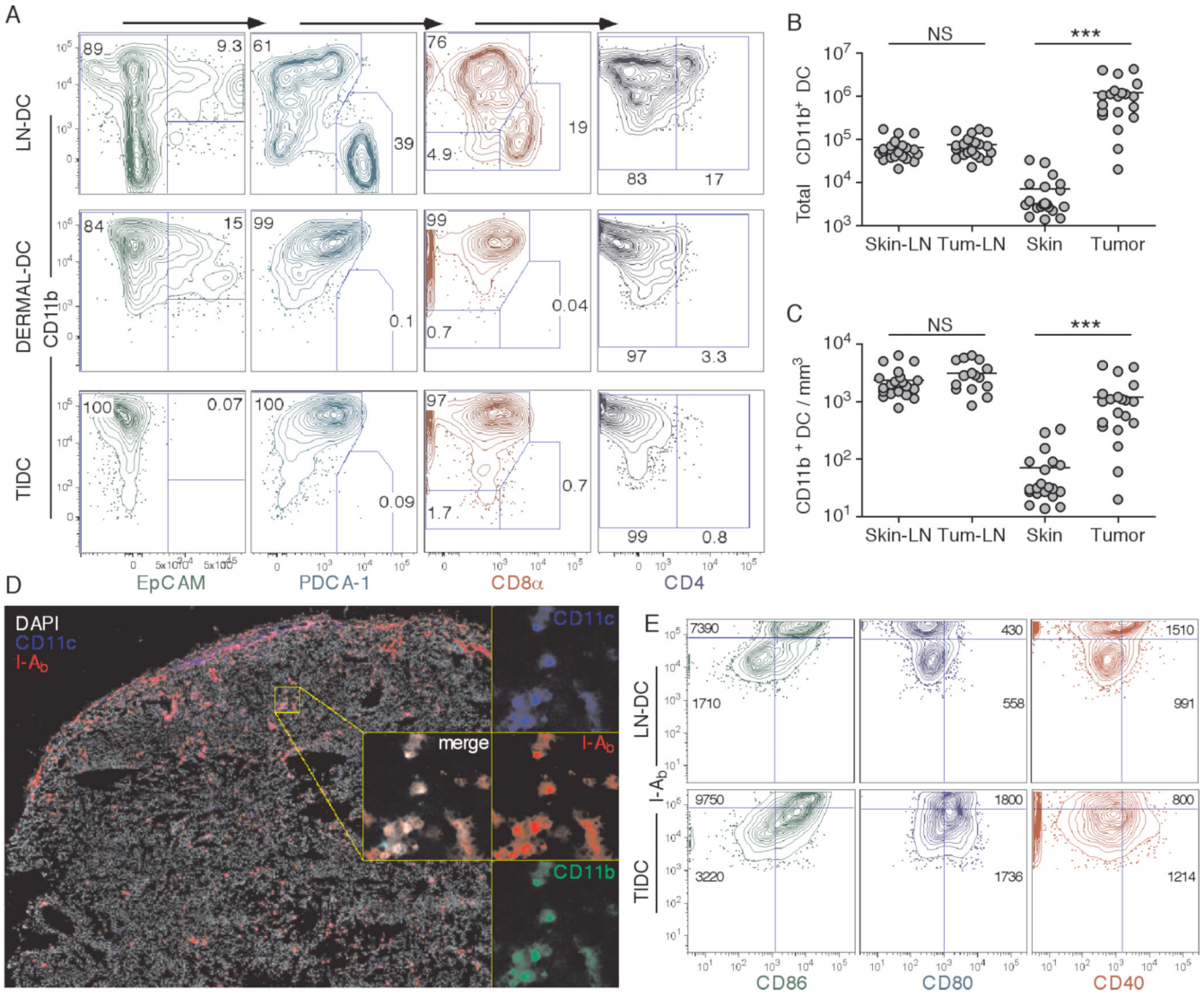


**Figure 2.**

Characterization of tumor infiltrating DC (TIDC). Skin DLN and dermal DC, as well as B16.F10 TIDC ($CD3^{-}CD19^{-}CD11c^{+}I\text{-}A_b^{+}$) were analyzed for expression of EpCAM, PDCA-1, CD8α and CD4 in a series of progressive gating plots (A). Numbers in the plots indicate percent cells in respective gate. Skin DLN, B16.F10 DLN, $1\times2cm^2$ patch of skin, and day-12 B16.F10 tumors were harvested and analyzed for the total number of $CD11b^{+}$ DC (B), and their approximate tissue density (C). B16.F10 frozen tissue sections were examined for CD11c, $I\text{-}A_b$ and DAPI staining (left), and for co-localization of CD11c, $I\text{-}A_b$, and CD11b (zoomed-in and merge insets, right) (D). Expression of $I\text{-}A_b$ vs. CD86, CD80 and CD40 was examined on $CD11b^{+}$ LN DC and TIDC (E). Numbers in the plots indicate MFI of the analyzed marker for either the $I\text{-}A_b^{+bright}$ (top) or $I\text{-}A_b^{+dim}$ (bottom) population. Data are representative of at least two independent experiments.

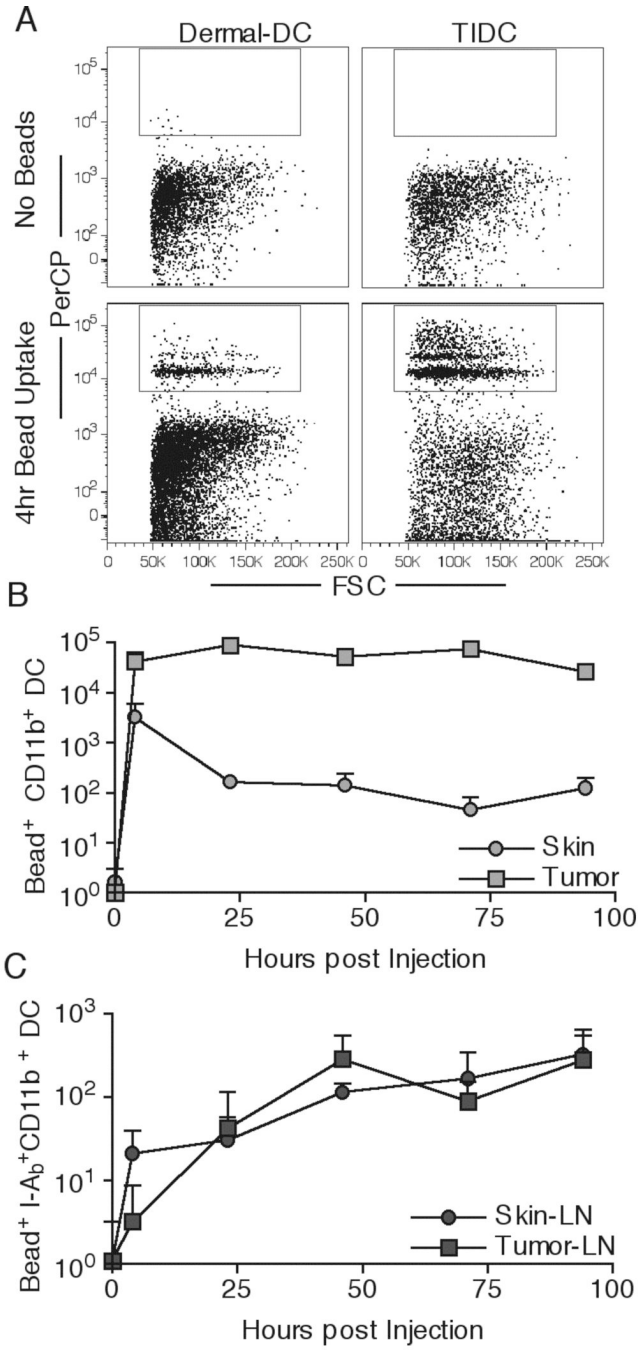


**Figure 3.**

TIDC exhibit reduced *in vivo* migration to draining LN. $5\times10^8$ red fluospheres were injected s.c. into naïve or i.t. into B16.F10-bearing animals. Dermal DC and TIDC were examined for the ability to pick up beads 4hr post injection (A). Total numbers of Bead+ CD11b+ DC at the injected skin site or the tumor were quantified at the indicated times (B). Total numbers of migratory DC (Bead$^+$ I-A$_b{}^{+\text{bright}}$ CD11b$^+$) in draining LN were quantified (C). Data are representative of three independent experiments.

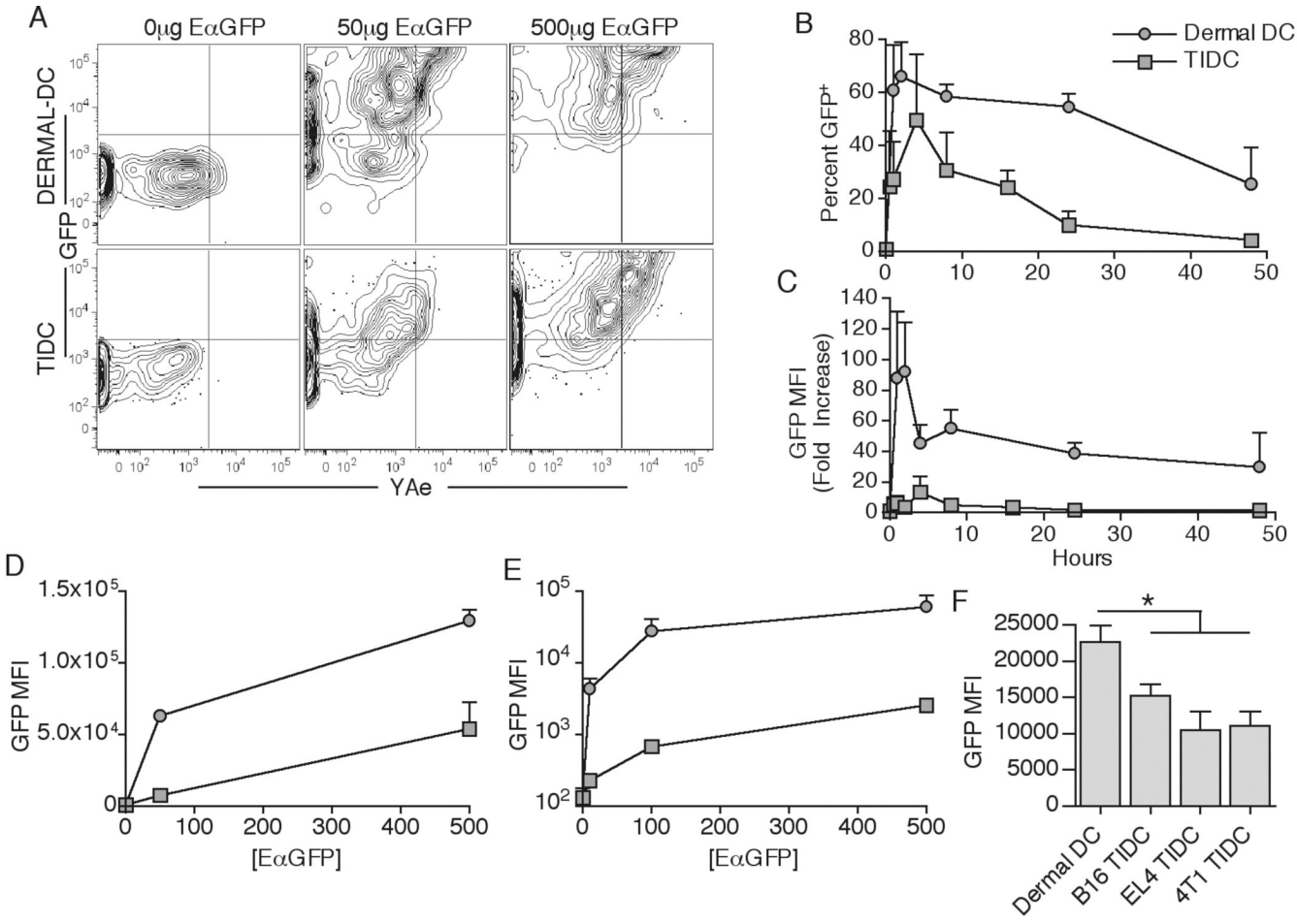


**Figure 4.**

TIDC are intrinsically defective in Ag uptake. 50μg or 500μg of EαGFP (same volume) was injected either s.c. into naive or i.t. into B16.F10-bearing animals. Dermal DC and TIDC were examined for GFP fluorescence and YAe antibody staining 3 and 4hr, respectively, post injection (A). Percent GFP $^{+}$ (B) and fold increase in GFP MFI from no injection control (C) for dermal DC and TIDC were quantified at indicated times post injection of 50μg of EαGFP. Dermal DC and TIDC were examined for GFP MFI 3 and 4hr, respectively, post injection of indicated quantities of EαGFP (D). DC were magnetically isolated and plated *in vitro* with indicated doses of EαGFP for 45 min at 37°C. Cells were then examined for intracellular GFP fluorescence (E). Tumor-free, B16.F10-bearing, EL4-bearing, and 4T1-bearing animals were injected with 50μg EαGFP. GFP MFI for dermal DC and TIDC was quantified 4hr after injection (F). Data are representative of at least two independent experiments.

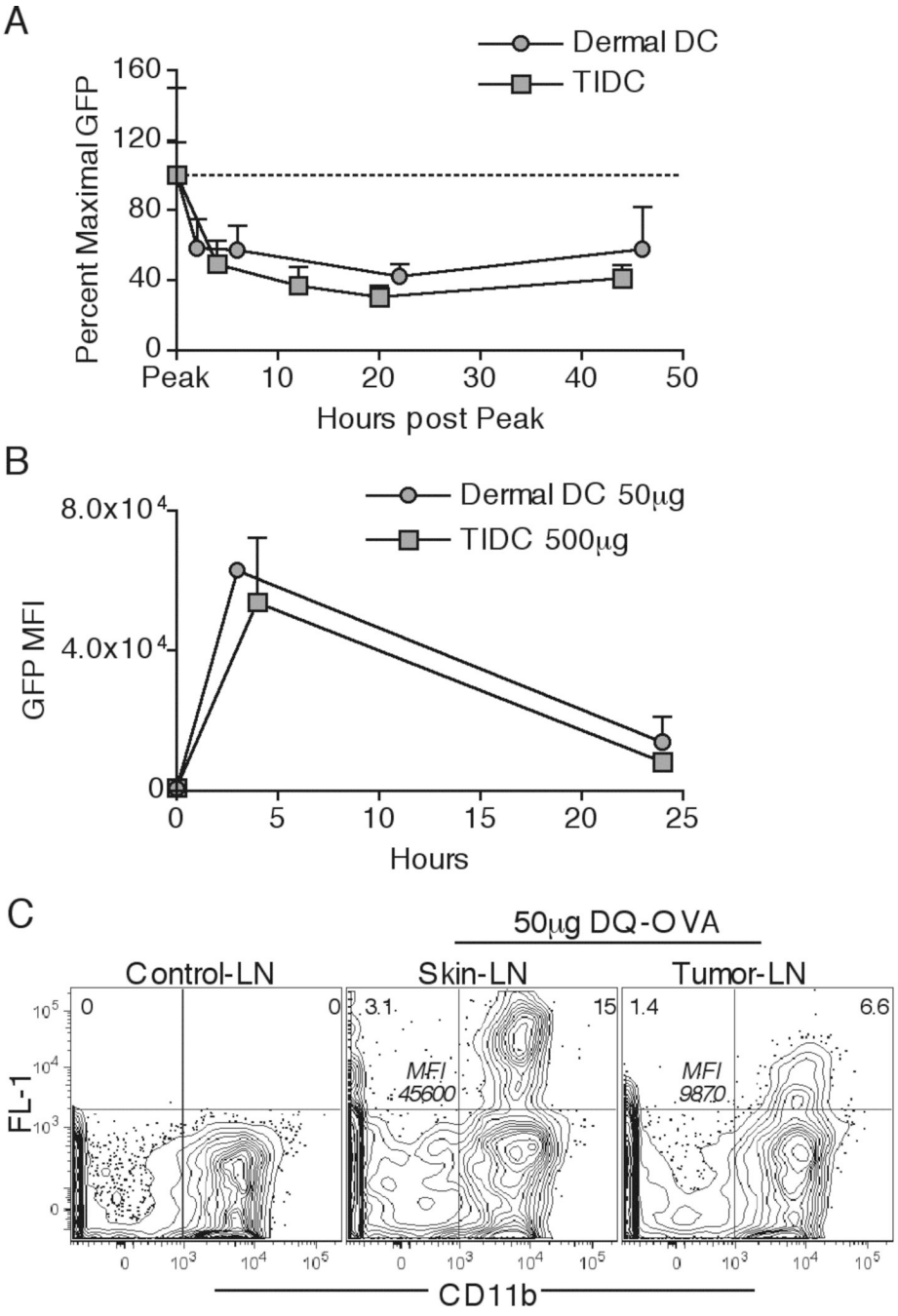


**Figure 5.**

Dermal DC and TIDC exhibit similar protein degradation kinetics. 50μg of EαGFP was injected either s.c. or i.t. Peak of EαGFP uptake was found by identifying the time post injection when the DC had the maximal GFP MFI. Dermal DC and TIDC were analyzed for their GFP fluorescence as a percent of maximal GFP MFI at various times post the peak of uptake (A). Dermal DC and TIDC were examined for GFP MFI at indicated times post s.c. injection of 50μg and i.t. injection of 500μg EαGFP (B). 50μg of DQ-OVA was injected either s.c. or i.t. Draining LN DC were examined for cells exhibiting FL-1 fluorescence and expressing the CD11b marker 24hr post injection (C). Numbers in top corners indicate percent cells in respective quadrant. Numbers in the center of the plot indicate FL-1 MFI for the $CD11b^+$

Fl-1$^+$ population. Data are representative of at least two independent experiments, with the exception of detailed dermal DC degradation kinetics (n=3 per time point).

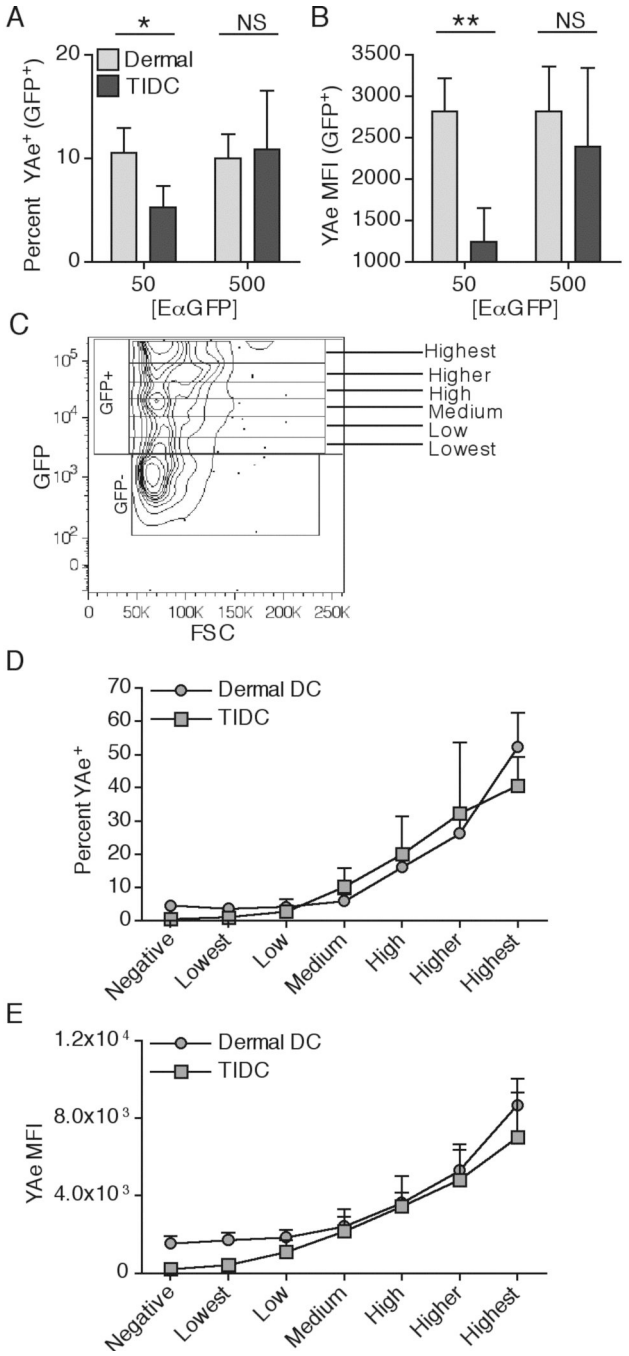


**Figure 6.**

Dermal DC and TIDC are intrinsically similar in MHC-II presentation. 50μg of EαGFP was injected either s.c. or i.t. Percent $YAe^+$ (A) and YAe MFI of the $GFP^+$ population (B) was quantified in dermal DC and TIDC 3 or 4 hr, respectively, post injection. Gating strategy for separating cells by the level of intracellular GFP is shown (C). Dermal DC and TIDC were examined for the percent $YAe^+$ (D) and YAe MFI after separation into indicated $GFP^+$ populations. Data are representative of at least three independent experiments.

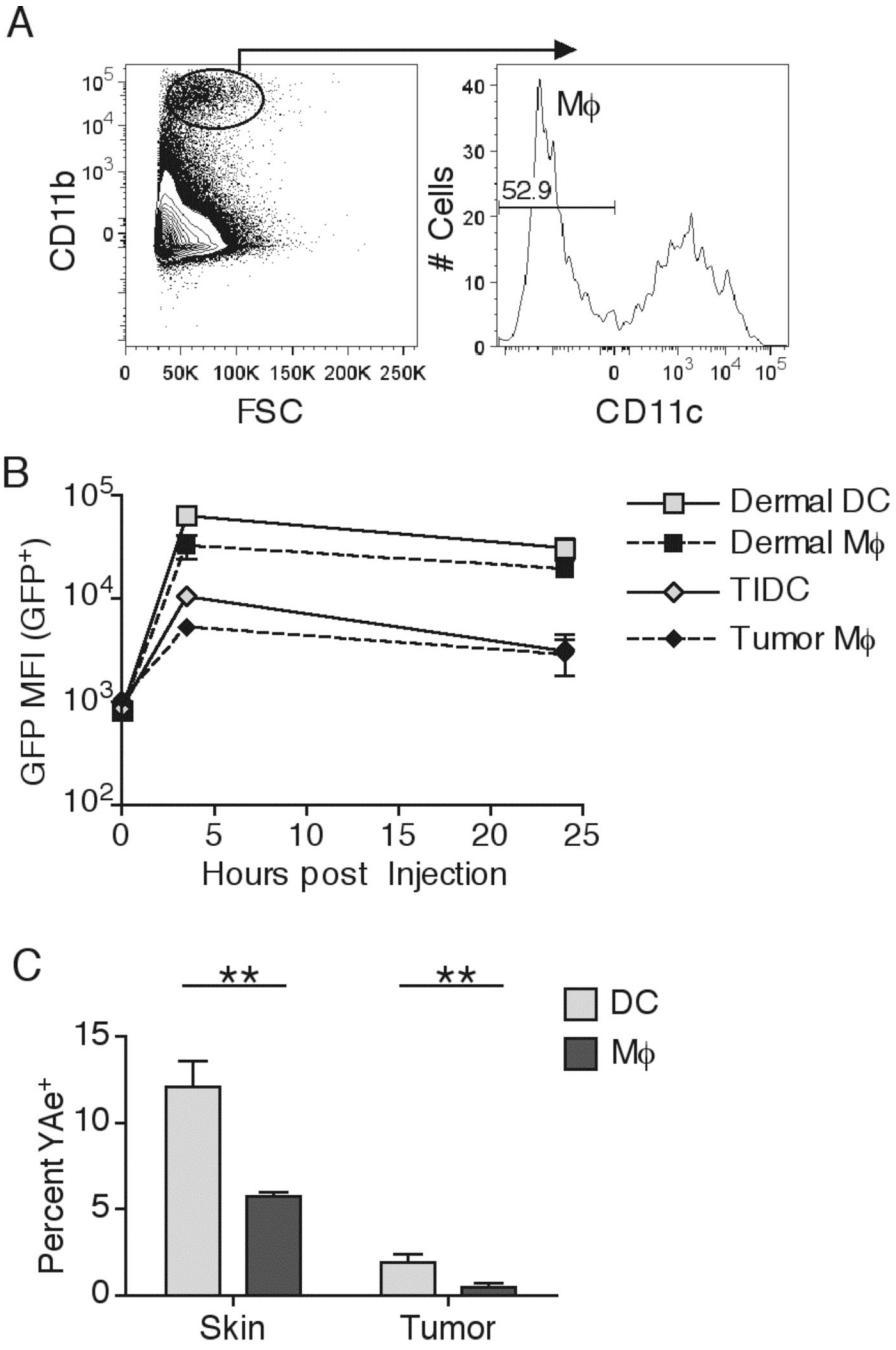


**Figure 7.**

Dermal and tumor infiltrating macrophages are inefficient at MHC-II presentation. 50μg of EαGFP was injected either s.c. or i.t. Macrophage (Mφ) populations were examined by gating on $FSC^{larger}CD11b^{+}CD11c^{-}$ cells (A). Number in the plot indicates the percent of Mφ in the total $CD11b^{+}$ population in a representative B16.F10 tumor. $GFP^{+}$ DC and Mφ populations were compared for intracellular GFP MFI at indicated time points (B). Skin and tumor DC and Mφ were examined for percent $YAe^{+}$ cells 4hr post injection (C). Data are representative of three independent experiments.

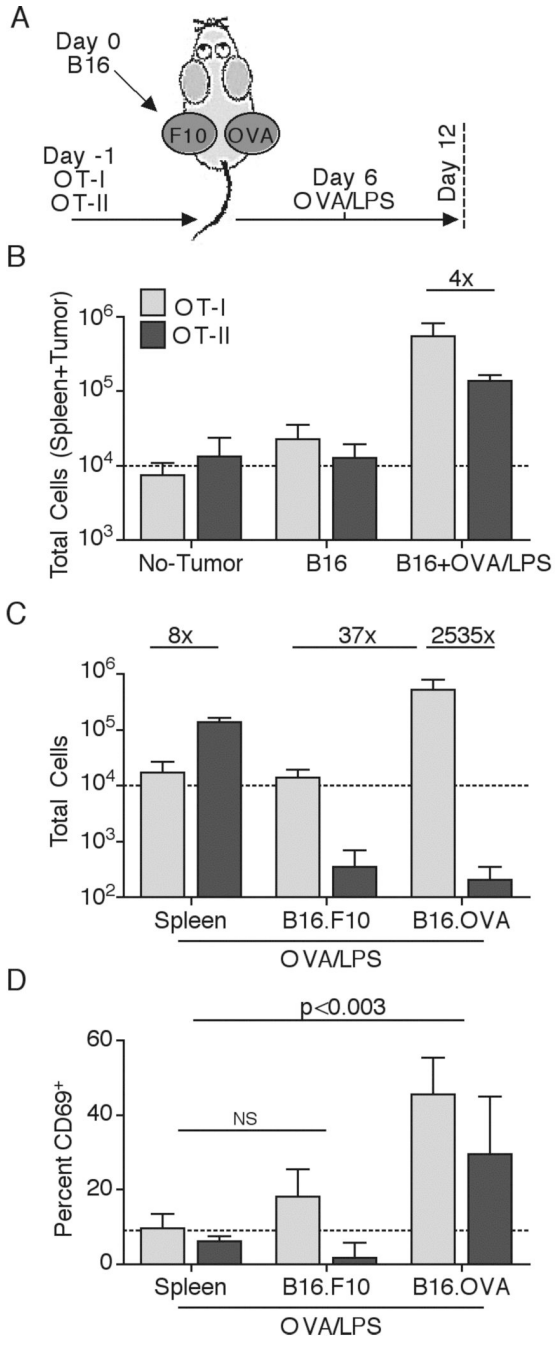


**Figure 8.**

CD4 T cell exhibit poor ability to infiltrate tumors in Ag-dependent and –independent manner. Naïve OT-I and OT-II T cells were transferred into animals some of which received a double-sided inoculation with B16.F10 and B16.OVA melanoma one day later. Some of the animals were immunized with OVA/LPS 6 days after. All mice were sacrificed 12 days post tumor injection (A). Total numbers of OT-I and OT-II T cells in collected tissues (two tumors + spleen) were compared for different groups (B). Immunized animals were examined for total numbers of OT-I and OT-II T cells in the spleen, B16.F10 and B16.OVA tumors (C). Numbers indicate fold difference in cell number between compared populations. Percent $CD69^+$ of the

total population was quantified for OT-I and OT-II T cells found in the spleen and two tumors in immunized animals (D). Data are representative of at least two independent experiments.

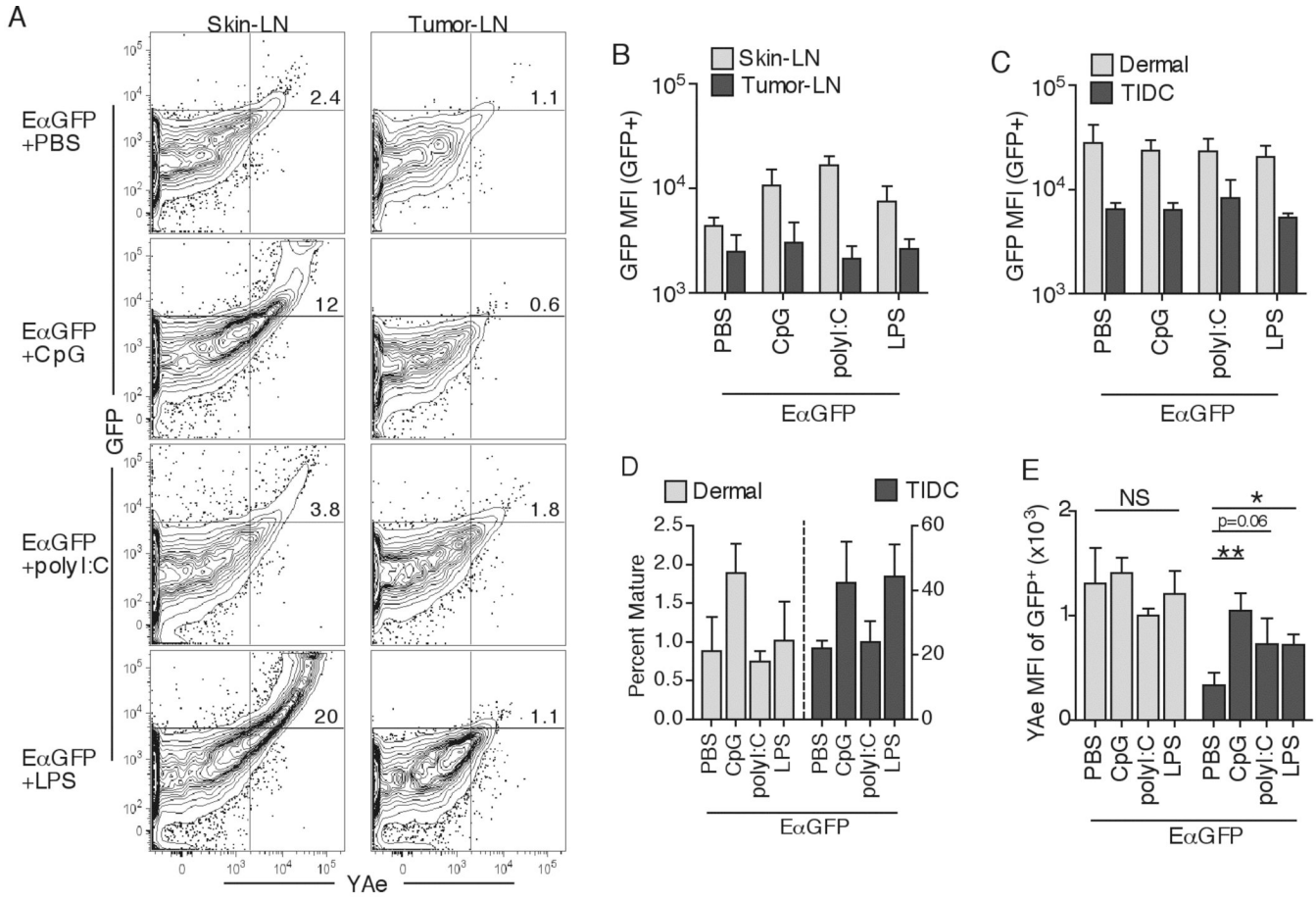


**Figure 9.**

Adjuvant mediated TIDC maturation does not influence Ag uptake. 50μg of EαGFP alone, or with CpG, polyI:C, or LPS (same volume) was injected either s.c. or i.t. $CD11b^+$ DC in DLN were examined for GFP fluorescence and YAe antibody staining 24hr later (A). Numbers in the plots indicate percent cells in the top right quadrant. GFP MFI of $GFP^+CD11b^+$ DC in DLN samples was quantified (B). GFP MFI of $GFP^+$ dermal DC or TIDC was quantified 4hr post injection (C). Percent fully mature DC ($I\text{-}A_b{}^{+bright}CD86^+$) 4hr post injection was quantified (D). $GFP^+$ dermal DC and TIDC were examined for percent $YAe^+$ cells 24hr post injection (E). Data are representative of two independent experiments.